Title: Controlled Release Tests Results for the Methane Lidar Camera

Authors: Manasi Doshi* (mdoshi@slb.com), Tetsushi Yamada*, Scott Quinn*, Gokhan Erol*, Christopher Boucher*, Michael Kenison*, Andrew E. Pomerantz*

Author Affiliations: *SLB Technology Corporation

This paper is a non-peer reviewed preprint submitted to EarthArXiv

Controlled Release Tests Results for the Methane Lidar Camera

Manasi Doshi* (mdoshi@slb.com), Tetsushi Yamada*, Scott Quinn*, Gokhan Erol*, Christopher Boucher*, Michael Kenison*, Andrew E. Pomerantz*

*SLB Technology Corporation

Abstract

Methane emissions detection using continuous monitors enables round-the-clock monitoring to quickly identify emissions from oil and gas facilities. The SLB methane lidar camera participated in Stanford University's 2024 Methane Controlled Release Campaign to characterize its performance at detecting, localizing, and quantifying methane emissions from different sources. The camera successfully detected and localized emissions as low as 0.3 kg/h as well as super emitters as high as 310 kg/h. The camera detected all but one emission greater than 1 kg/h, resulting in a limit of detection at 90% confidence of 1.5 kg/h. In addition, the camera localized all emissions to the correct piece of equipment or to the adjacent piece of equipment, including many releases where the camera's vantage point was suboptimal. The emission rates measured by the camera showed a systematic underestimation compared to the ground truth results. Such an underestimation is unexpected and inconsistent with the camera's performance in previous studies. In this paper, we perform a root cause analysis to identify the cause of the underestimation. The analysis concludes that the measured methane signal was accurate and that the underestimation was caused by a wind shadow that resulted in the camera's anemometer systematically underestimating the wind speed. Reprocessing the methane lidar camera's data using an on-facility anemometer not affected by a wind shadow instead of the camera's anemometer resulted in quantification that was within a factor of two 78% of the time and a systematic bias of 11%. The 90% limit of detection, the fraction of results within a factor of two, and the systematic bias (using the on-facility anemometer), are superior to any scanning/imaging system at METEC 2023 and 2024 ADED programs. As a result of this study, improvements in the camera installation workflow have been introduced to avoid wind shadows in the future.

Introduction

Methane is a potent greenhouse gas with global warming potentials up to 84 times that of carbon dioxide (Balcombe, et al., 2018; Pomerantz, et al., 2022). Methane emissions from oil and gas operations can range in magnitude from a few grams per hour to a few tons per hour (Curry, et al., 2022; Sherwin, et al., 2024). The majority of these methane emissions arise from episodic and abnormal sources that cannot be effectively reduced or quantified using periodic screening, and the short duration of these emissions implies that high sampling rate measurements like continuous monitors are required to establish accurate inventories of methane emissions (Wang, et al., 2022) . In an attempt to reduce the climate impact from oil and gas methane emissions, in 2024, the U.S. Environmental Protection Agency (EPA) proposed new regulations (EPA, 2024) permitting the use of continuous methane monitoring systems for regulatory compliance. The regulations define reporting requirements and lower limits of detection that continuous monitors need to meet before they can be permitted for use by the EPA. The minimum detection threshold is set to 0.4 kilograms per hour (kg/h) for fugitive emissions detection, and short- and long-term action levels are defined based on the rolling-window-averaged mass emission rate. Continuous monitors can also be used to determine the duration of large release events, which are often

unpredictable and can happen in-between LDAR (leak detection and repair) or aerial detection campaigns.

To establish the detection and quantification capabilities of continuous methane monitors, several academic institutions have conducted single-blind controlled methane release tests (Bell, et al., 2017; Bell, 2023; Bell, et al., 2022; Sherwin, 2021; Sherwin, 2023). These tests either simulate the emissions profiles of oil and gas facilities or are conducted at actual facilities. In addition to field tests, the SLB methane lidar camera (SLB, 2022) has participated in various blind tests to define its operating thresholds.

The methane lidar camera is a continuous methane monitoring system that employs laser absorption spectroscopy and lidar measurements to detect, localize, and quantify methane emissions. The camera uses a mass balance equation to quantify the emission rate where the emission rate is directly proportional to the flux of methane through a cross section of a plume and the wind velocity component along the plume. Like many methane monitors, the mass emission rate determined by the methane lidar camera depends sensitively on both the measured methane signal and the measured wind speed and direction. The lower limit of detection of the camera is established at 0.4 kg/h via blind testing at Colorado State University's Methane Emissions Technology Evaluation Center (METEC) Advancing Development of Emissions Detection (ADED) (Ilonze, et al., 2024; Andrews, et al., 2023; Doshi, 2024) and the camera is capable of identifying emissions with 100+ kg/h magnitude.

In September 2024, the SLB methane lidar camera participated in Stanford University's Methane Controlled Release Campaign conducted at the TotalEnergies Anomalies Detection Initiatives (TADI) facility in France. The facility has 12 release points from oil and gas equipment, including tanks and wellheads, all shown in Figure 1(a). The camera was installed at the northwest corner of the facility on a pole attached to the walkway railing of a tank, approximately 10 m above ground, as shown in Figures 1(b) and 1(c), and the camera's anemometer was attached on a separate pole about 9 m above ground. This installation setup is nonstandard for the camera. The standard commercial installation location for the camera is atop the SLB custom-designed tower between 15 and 17 m in height at a location optimized based on the facility layout and the geometries of the various equipment, with the anemometer located at ~1.5 m high above ground on a protruding arm. The height specification and tower design were ascertained based on the following factors: (1) installing the camera at an elevation above ground of between 15 and 17 m ensures that the camera is located above most equipment at a typical oil and gas facility. Doing so provides a direct line of sight from the camera to equipment of interest while simultaneously allowing the ground to be used as a reflecting surface for the camera's laser beam to diffuse off; (2) A majority of oil and gas emission sources are between ground and ~3 m high. The anemometer installation height of 1.5 m ensures that the wind speed measured is representative of the emission plume speed. Installing the anemometer too high or too low can introduce systematic errors in the methane emission rate quantification by the camera since wind speeds increase with height according to a power law approximation (Hanna, et al., 1982) and (3) installing the anemometer on a protruding arm ensures that the anemometer is in free space and not in the wind shadow of any structure or equipment at the facility. Due to facility restrictions on allowed installation locations at TADI, the anemometer had to be installed unusually close to the aforementioned tank and at a much higher height than standard installations, while the camera had to be installed at a much lower height.

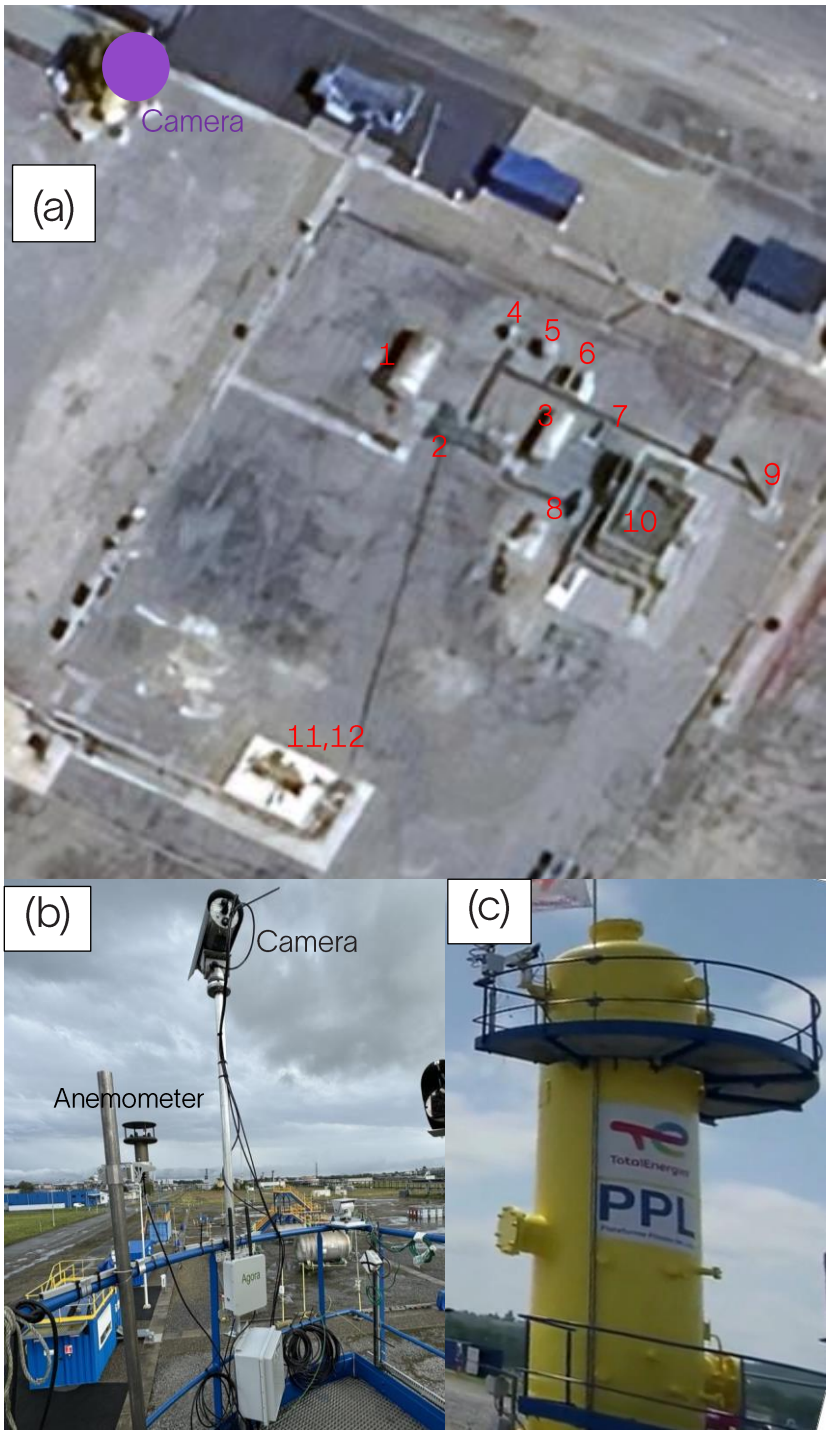

Figure 1: (a) Satellite image of the TADI facility showing 12 potential release sources. The camera was installed in the purple circled region in the northwest. (b) Camera and its anemometer installed on poles extended from the walkway railing of the tank shown in (c). Image (c) is from TADI's website (Total Energies, 2025)

Results and Discussion

During the Summer 2024 Methane Controlled Release Campaign, Stanford conducted 78 release experiments with emission rates varying between 0.02 and 310 kg/h. Each emission was about 45 minutes in duration with at least 15 minutes between consecutive emissions. Participating teams including SLB were not informed about the release location or release magnitude. The release experiments included four zero-volume releases; i.e., no methane was actually released during those four experiments. For each controlled release event, participating teams reported to Stanford whether the emission had been detected, where the monitor localized the source of the emission, and how large the monitor quantified the rate of the emission. Once all teams had submitted their data, Stanford distributed information on their methane release schedule along with the release location and release rate.

Figure 2 shows some emissions as seen by the camera. Each image is an overlay of the methane concentration measured by the camera on the signal count (top-right). The overlay images help with emission source identification, enabling facility operators to take very quick emissions mitigation measures.

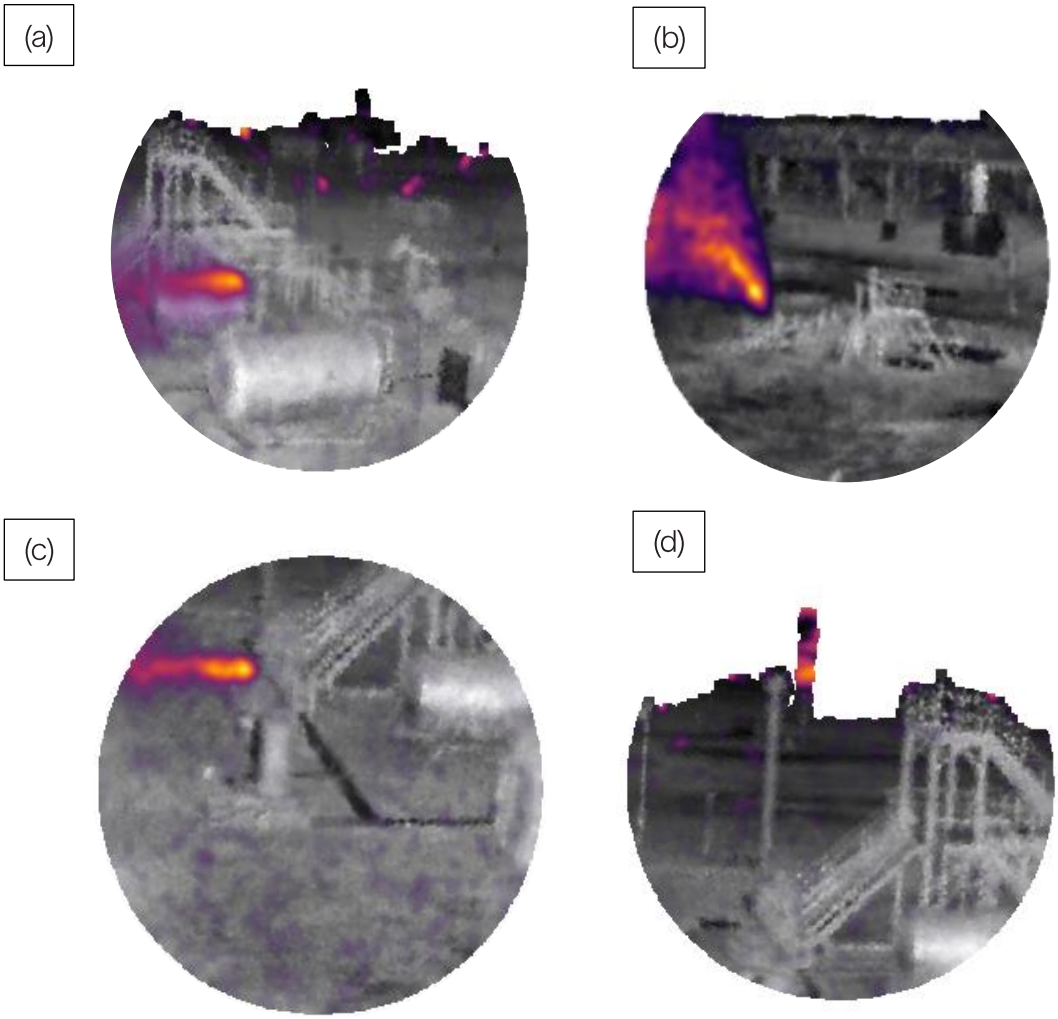

Figure 2: Images from the camera: (a) shows an emission from a tank, (b) shows a large emission, (c) shows emissions from one of the three inline sources (RPB, scrubber, product skid) at TADI from the camera's point of view, and (d) shows the

camera's perspective of the 6.5-m flare. Due to the unusually low height of the camera at TADI, the relative height of the flare with respect to the camera often does not provide a background scattering surface to confidently detect emissions.

Detection

Figure 3 shows the emissions detected (green) and not detected (red) by the camera. The dashed line indicates 0.4-kg/h emission rate: the lower limit of detection of the camera as well as EPA's minimum detection threshold for continuous monitors. As shown in the figure, the camera detected emissions as low as 0.3 kg/h (exceeding the EPA's requirement of 0.4 kg/h) and higher than 300 kg/h. The camera detected all but one emission with a rate greater than 1 kg/h. The camera missed one emission of about 20 kg/h from a flare that was too tall for the camera's nonstandard height and location—there was no reflecting surface behind the flare for the signal to return to the camera, as shown in Fig. 2(d).

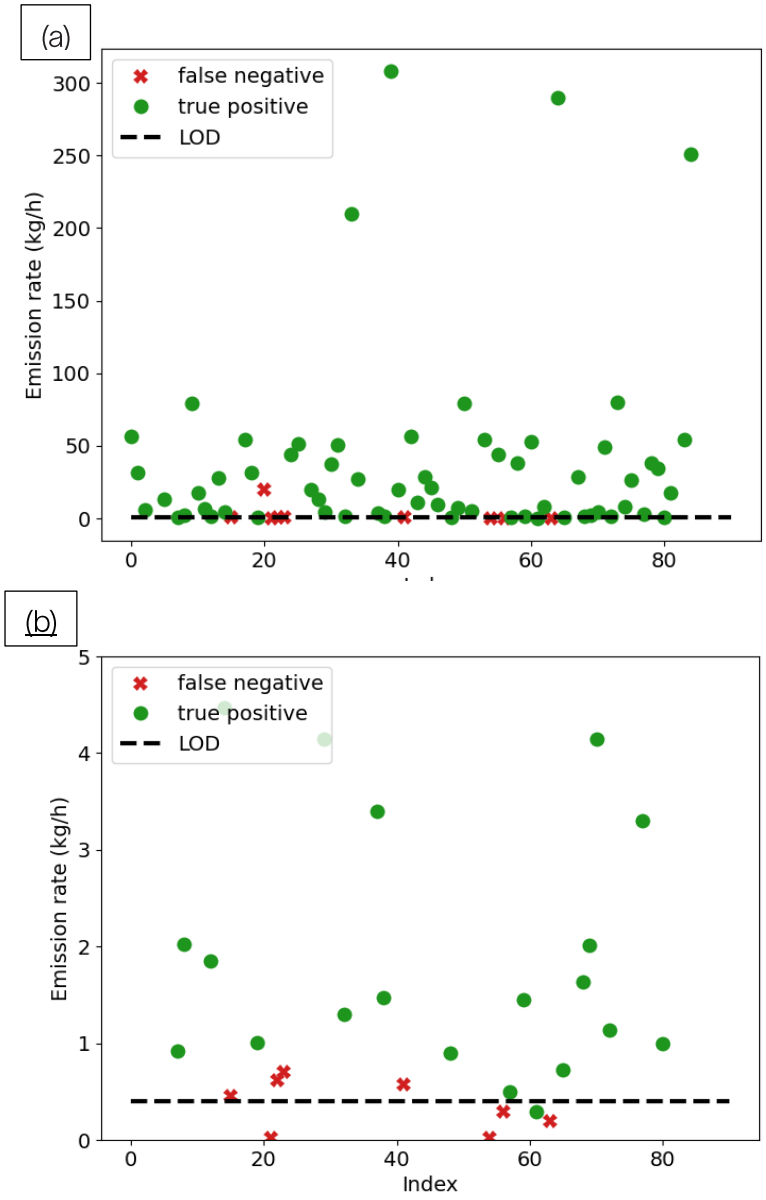

Figure 3: Plots showing the emissions detected (green) and not detected (red) by the camera over a full range of release rates in (a) and zoomed in for release rates below 5 kg/h in (b). LOD = limit of detection.

Table 1 shows a confusion matrix showing the releases that were successfully detected as emissions (true positives; TP) or blanks (true negatives; TN), missed (false negatives; FN), or detected excessively (false positives; FP). Almost all the false negatives are below or close to the lower limit of detection of the camera as shown in Fig. 3(b) and the one false positive was quantified at 0.2 kg/h—well below the action level set by the U.S. EPA.

Table 1. Confusion matrix showing the detections by the camera.

	Released	Not released
Detected	64 (TP)	1 (FP)
Not Detected	10 (FN)	4 (TN)

Figure 4 shows the probability of detection (POD) curve showing the fraction of emissions detected for specific emission rate bins. To calculate the 90% POD, we fit an exponential curve through the binned data. The limit of detection (LOD) at 90% POD for the camera equals 1.5 kg/h. As shown in the figure, the camera detects almost all the emissions greater than 1 kg/h, but the one missed detection at the flare at about 20 kg/h increases the LOD to 1.5 kg/h. If the camera had been installed in its standard way (at its usual height and at an optimized location), this emission was unlikely to be missed and the limit of detection would likely be lower. Even including that point, the 90% LOD observed here for the methane lidar camera was better than any scanning/imaging system included in the (Ilonze, et al., 2024) or 2024 (Cheptonui, et al., 2024) METEC ADED tests.

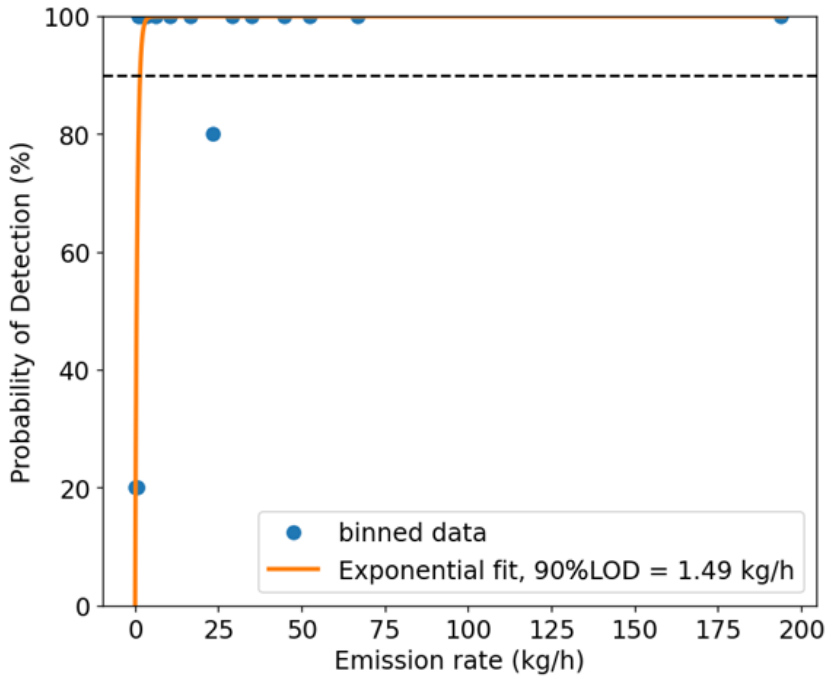

Figure 4 : Probability of detection against controlled release rate. Including the false negative resulting from the nonstandard camera height, the 90% detection limit is 1.49 kg/h.

Localization

Once an emission is detected, the lidar camera system has algorithms that determine the emission source. When the camera has a direct line of sight to an emission, it can identify the emission source with full confidence. If the emission plume originates at a source that is obstructed from the camera's point of view or if there are multiple sources in line [as shown in Fig. 1 (c)], the camera considers the equipment in the foreground to be the source. During the Stanford tests, even with multiple inline and obstructed sources, the camera identified the correct emission source 69% of the time and attributed the emission to the second nearest source 31% of the time, as shown in Fig. 5. Such accurate and precise emission source identification makes it easier for repair crews to quickly fix emissions.

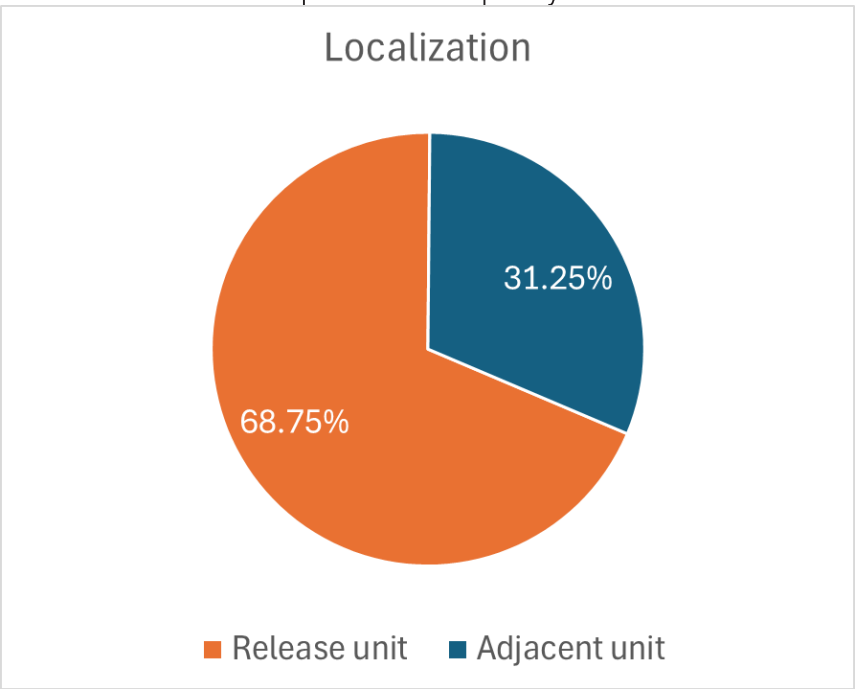

Figure 5: Localization accuracy of the camera. Even though the TADI facility is complex, with multiple pieces of equipment within a couple of meters of each other and a camera installation at an unusually low height, 69% of the emissions were localized to the correct equipment unit and all other emissions were localized at the adjacent equipment unit.

Quantification

The system combines methane concentration data acquired via the lidar camera with wind data acquired via an anemometer connected to the camera to quantify the methane emission rate. Figure 6 shows the quantification by the camera versus Stanford's release rate. The camera has a 1-sigma factor uncertainty of 2.0 for its quantification; i.e., quantified emission rates are within a factor of two of the real emission rate for one standard deviation of the emissions. The camera showed a systematic underestimation for emission rate quantification during the Stanford tests. Such underestimation is uncharacteristic for the camera based on METEC tests (Ilonze, et al., 2024) (the methane lidar camera is Solution B) and our internal studies (Andrews, et al., 2023).

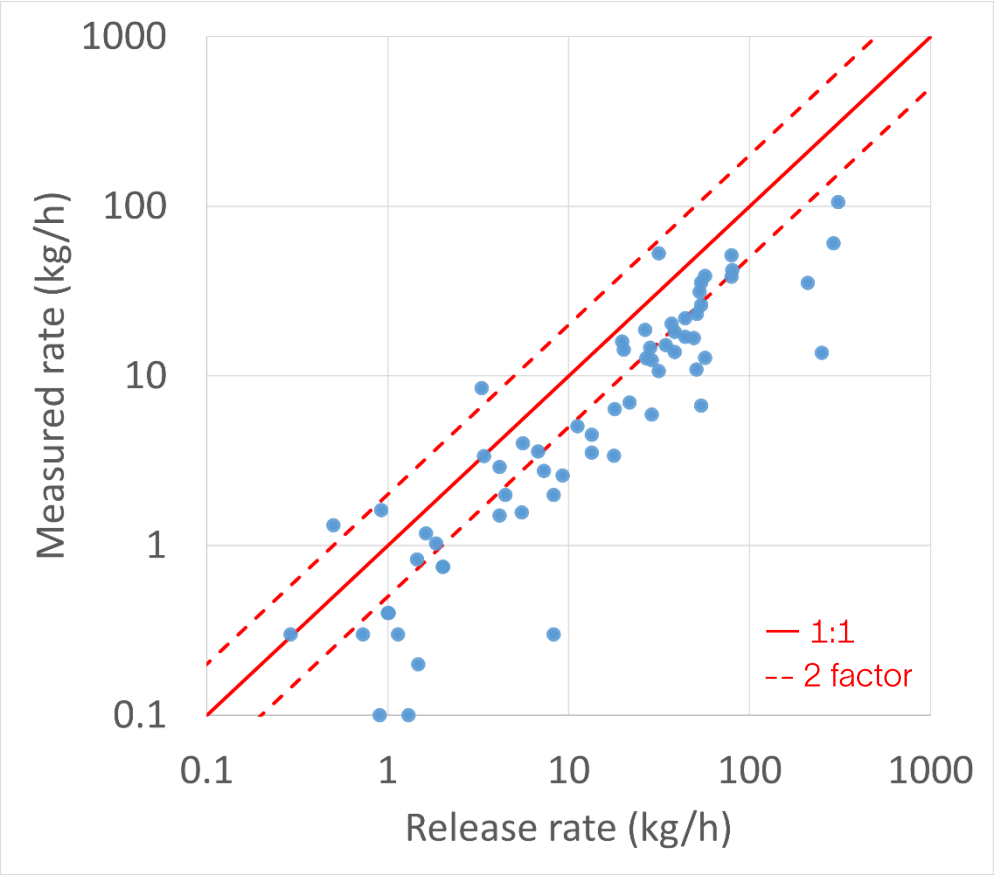

Figure 6: Preliminary quantification by the lidar camera shows a systematic underestimation bias.

The emission rate quantification by the camera depends on the methane concentration measured by the camera and the wind velocity measured by the anemometer. To understand the root cause of the bias, we systematically analyzed the potential causes of such underestimation. Before installation, the camera undergoes a few quality control checks, to prevent inaccuracies with methane concentration measurements. The checks include a test using a reference methane balloon to ensure that the camera reads methane concentration values correctly. The camera is equipped with a sealed gas cell precalibrated with a known concentration of methane to ensure that the laser's wavelength is locked in around the methane absorption wavelength. We confirmed that the camera used for the Stanford tests had passed these checks prior to the tests. We also ensured that the absorption spectra collected by the camera during the Stanford tests are as expected. The results from these checks ruled out the possibility of incorrect methane concentration measurements.

Wind Analysis

Since the emission rate computed by the camera is directly proportional to the wind speed along the emission plume, we compared the wind speeds and directions measured by the camera anemometer to those measured by TADI's anemometer that Stanford used for their own analysis. The TADI facility has a lidar anemometer that measures wind velocity between 10- and 300-m heights above ground. The camera anemometer was installed at ~9-m height above ground so all wind comparisons in this paper are made against the 10-m measurements by the TADI anemometer to avoid effects from increasing wind speeds at higher elevations. Figure 7 shows a comparison of the wind speeds (top) and directions

(bottom) measured by the two anemometers resampled to the same measurement frequency. The wind directions represent the direction from which the wind originates where 0° is winds originating from the north and 90° is winds originating from the east. Measurement errors for the sonic anemometer used by the camera are less than +/- 2% for wind speeds and wind direction (Gill Instruments Ltd., 2024). Here, wind speeds and directions measured by the camera's anemometer and by TADI's anemometer differed by much more than those typical measurement errors. That difference suggests one anemometer was in a wind shadow, where a nearby obstacle partially blocks the wind.

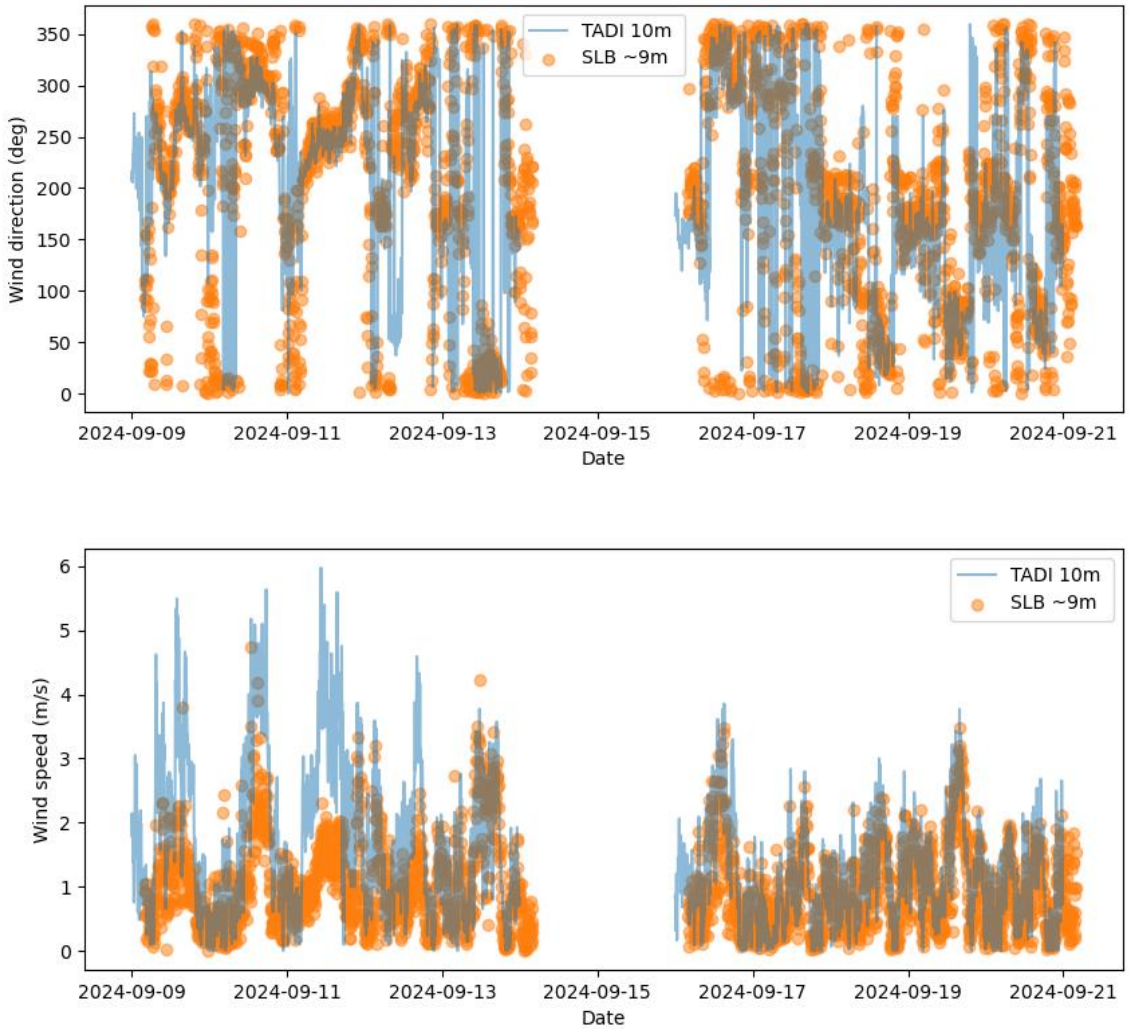

Figure 7: Plots comparing the wind direction (top) and wind speed (bottom) measured by the camera anemometer and the anemometer at TADI used by Stanford.

Figure 8 explores the differences between the camera's anemometer and TADI's anemometer in more detail by evaluating correlations between measured wind speed and measured wind direction. At some wind directions, similar wind speeds are measured by both anemometers. However, when the wind is blowing at a direction around 250°, the wind speeds measured by the camera's anemometers are lower than the wind speeds measured by TADI's anemometer.

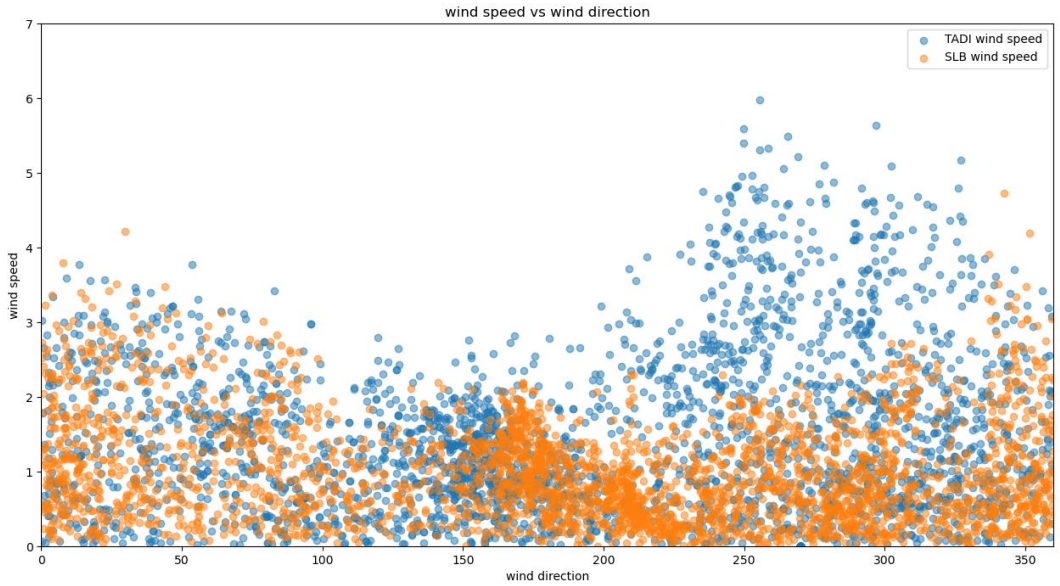

Figure 8: Wind speeds measured by the camera and the TADI/Stanford anemometer as a function of the measured wind direction. Plot shows significant differences in measurements around 270°.

The tank next to the camera and anemometer has a large outlet pipe coming out of the top and going behind the tank in Figure. 1(c). The top of the yellow tank is about 1 to 2 ft taller than the anemometer height. The anemometer is within 1 m of the tank horizontally. These geometries, distances, and height differences create a complex system where multiple parallel effects including wake and downwash combine to form interesting flow patterns. Figure 9 shows the relative positions of the tank, the camera, and the anemometer. The tank extends from about 230° to 280°, blocking winds originating from those directions. As shown in Fig. 8, the wind speeds are significantly impacted for the same direction range, peaking around 250°, confirming a wind shadow effect from the tank on the anemometer.

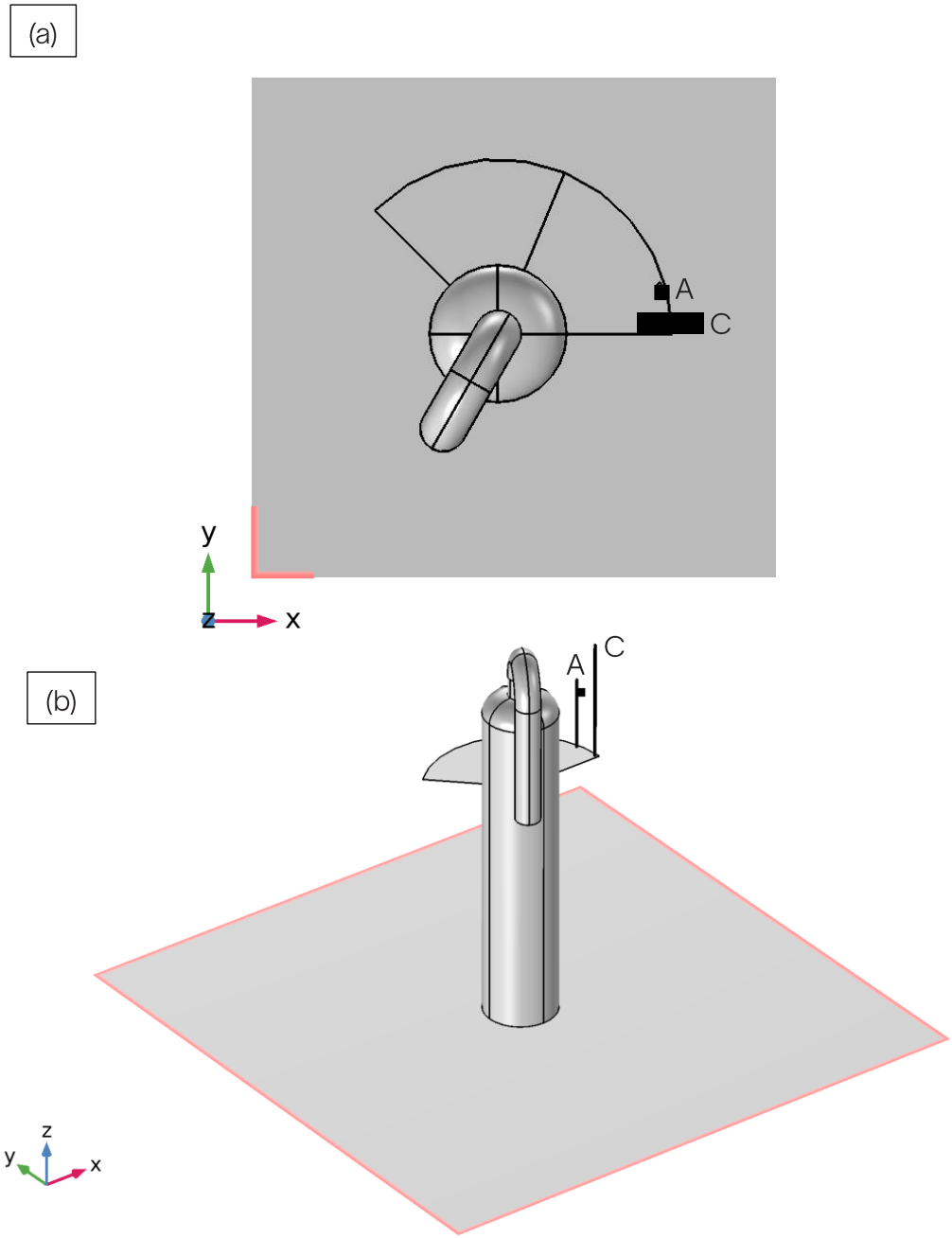

Figure 9: Schematic of the top view (a) and the 3D view (b) of a rendering showing the relative positions of the camera (marked by C), the anemometer (marked by A) and the yellow tank. X axis is pointing east (90°) and Y-axis is pointing north (0°).

Data Reprocessing

The mass emission rate determined by the methane lidar camera depends on both the methane data and the wind speed and direction. The wind speed and direction relevant for this approach are those experienced by the methane plume. The emissions sources and methane plumes at TADI are all in free

space, so the wind velocity measurements from TADI's anemometer (located in free space) are more representative than the wind velocity measurements from the camera's anemometer (located in a wind shadow). To mitigate the effects from this wind shadow, new emission rates were computed using the latest rate computation algorithm where the wind velocity data come from TADI's anemometer rather than the camera's anemometer. Wind measurements from TADI's anemometer were extrapolated to 2-m height by fitting a power law to the anemometer measurements between 10 and 300 m to ensure that wind speed is not overestimated at typical release heights. Figure 10 shows the recomputed emission rates as a function of Stanford's release rate. The emission rate measurements no longer have the bias introduced by underestimated wind speeds. This confirms that the wind shadow affected the anemometer measurements, thereby affecting the lidar camera's emission rate quantification. After reprocessing, 78% of the emissions are quantified within a factor of two of the release rate, outperforming the camera's specifications, with a mean bias of 11%, which is better than all scanning/imaging systems tested at METEC ADED 2023 (Ilonze, et al., 2024) or 2024 (Cheptonui, et al., 2024) tests.

These results indicate the importance of ensuring that the anemometer is installed in free space away from large structures and equipment that can influence the wind field locally. Following the Stanford tests, we added an additional step in our camera's installation workflow for nonstandard deployments with guidelines on identifying best locations for anemometer placement.

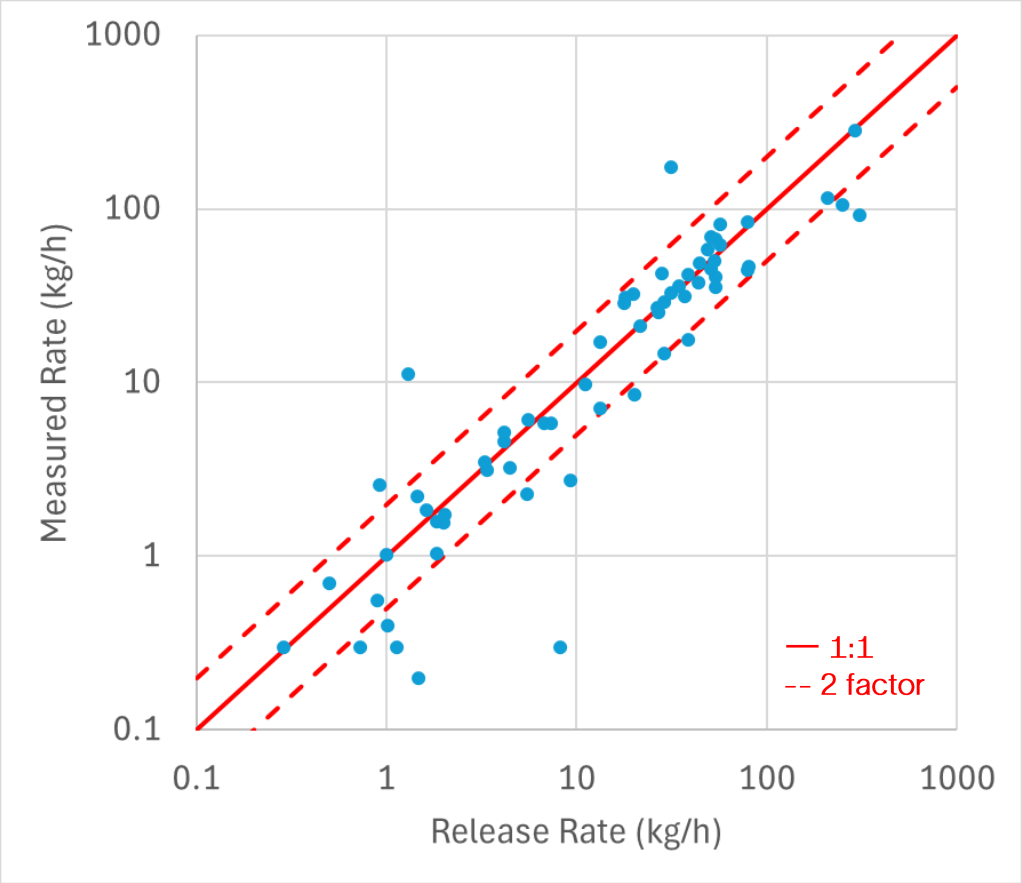

Figure 10: Reprocessed quantification by the lidar camera using wind velocity measured by TADI's anemometer shows that 78% of the emissions are quantified within a factor of two with a mean bias of 11%.

Conclusions

The SLB methane lidar camera participated in Stanford University's 2024 Methane Controlled Release Campaign. The camera successfully detected and localized emissions between 0.3 and 300+ kg/h. The limit of detection (1.5 kg/h at 90% probability) is better than any scanning/imaging instrument included in the 2023 or 2024 ADED tests at METEC. Even with a nonstandard installation, the localization accuracy (69% of emissions localized to the correct equipment group) is consistent with previous tests The preliminary emission rate quantification by the camera showed an unexpected systematic underestimation bias. During post-analysis, it was discovered that the wind speed measurements by the camera anemometer were much lower than TADI's anemometer used by Stanford, with the magnitude of the wind speed difference correlated to the wind direction. Due to unique constraints at TADI, the camera and anemometer were installed in a nonstandard manner, including being positioned unusually close to a large tank. We confirmed that these differences in measured wind speed and direction result from a wind shadow cast by the tank on the camera's anemometer. Recomputing the methane mass emission rates using TADI's wind measurements resulted in greatly improved performance: 78% of the rates were accurate within a factor of two, and the systematic bias was 11%, which is superior to any scanning/imaging instrument included in the 2023 or 2024 ADED tests at METEC. The key takeaway from the analysis is that the anemometer should be installed in free space where the wind field is not locally perturbed by structures at the facility. Based on these learnings, the camera and anemometer installation procedure was modified to avoid wind shadows in the future.

Acknowledgments

We appreciate Dr. Adam Brandt, Audrey McManemin, and the Stanford University team for including us in the 2024 Stanford Controlled Methane Release Experiment and for their support throughout the test process. We are also thankful to Catherine Juery and her team at TotalEnergies for their support during installation and testing. We are also grateful to Xiao Ai, Puneet Chhabra, and Murray Reed at QLM Technology Ltd. who provided valuable inputs during post-processing.

References

Andrews A. B. [et al.] Quantitative Mapping of Methane Emissions in Oil & Gas Facilities [Conference] // SPE Annual Technical Conference and Exhibition. - San Antonio : [s.n.], 2023.

Balcombe P. [et al.] Methane Emissions: Choosing the Right Climate Metric and Time Horizon [Journal] // Environmental Science: Processes & Impacts. - 2018. - Vol. 20. - pp. 1323-1339.

Bell C. [et al.] Comparison of Methane Emission Estimates from Multiple Measurement Techniques at Natural Gas Production Pads [Journal] // Elementa. - 2017. - 79 : Vol. 5.

Bell C. [et al.] Single-blind Determination of Methane Detection Limits and Quantification Accuracy using Aircraft-based LiDAR [Journal] // Elementa. - 2022. - 1 : Vol. 10. - p. 00080.

Bell C., Ilonze, C., Duggan, A., Zimmerle, D. Performance of Continuous Emission Monitoring Solutions under a Single Blind Controlled Testing Protocol [Journal] // Environ. Sci. Technol.. - 2023. - 14 : Vol. 57. - pp. 57 (14), 5794-5805.

Cheptonui F. [et al.] Assessing the Performance of Emerging and Existing Continuous Monitoring Solutions under a Single-blind Controlled Testing Protocol [Journal] // ChemRxiv. - 2024.

Curry T. [et al.] Benchmarking Methane and Other GHG Emissions of Oil & Natural Gas Production in the United States [Report]. - [s.l.] : Ceres, 2022.

Doshi Manasi Continuous Monitoring Systems for Complete Life Cycle Analysis of Methane Emissions [Conference] // ACS Fall 2024. - Denver : ACS SciMeetings, 2024.

EPA US Standards of Performance for New, Reconstructed, and Modified Sources in the Oil and Natural Gas Sector. 40 C.F.R. pt. 60, subpt. OOOOb. - 2024.

Gill Instruments Ltd. . Gill WindSonic M [Online]. - Gill Instruments Ltd., 2024. - 2 11, 2025. - https://gillinstruments.com/wp-content/uploads/2024/08/1405-0029-WindSonicM-issue-16.pdf.

Hanna S., Briggs G. and Hosker R. Handbook on Atmospheric Dispersion [Book]. - [s.l.] : U.S. Department of Energy, 1982.

Ilonze C. [et al.] Assessing the progress of the performance of continuous monitoring solutions under single-blind controlled testing protocol [Journal] // Environmental Science & Technology. - 2024. - 25 : Vol. 58. - pp. 10941-10955.

Pomerantz A. E. and Kleinberg R. L. Present Global Warming: A Justifiable and Stable Metric for Evaluating Short-lived Climate Pollutants. [Journal] // Environmental Research Letters. - 2022. - 11 : Vol. 17. - p. 114052.

Sherwin E. D., Chen, Y., Ravikumar, A. P., and Brandt,A.R. Single-blind Test of Airplane-based Hyperspectral Methane Detection via Controlled Releases [Journal] // Elementa. - 2021. - 1 : Vol. 9. - p. 00063.

Sherwin E. D., Rutherford, J. S., Chen, Y., Aminfard, S., Kort E. A., Jackson, R. B., Brandt, A. R. Single-blind Validation of Space-based Point-source Detection and Quantification of Onshore Methane Emissions [Journal] // Scientific Reports. - 2023. - Vol. 13. - p. 3836.

Sherwin E.D. [et al.] US Oil and Gas System Emissions from Nearly One Million Aerial Site Measurements [Journal] // Nature. - 2024. - Vol. 627. - pp. 328-334.

SLB Product sheet for LiDAR camera [Online]. - 2022. - 10 15, 2024. - https://www.slb.com/products-and-services/decarbonizing-industry/methane-emissions-management/sees-end-to-end-emissions-solutions-family/sees-methane-lidar-camera.
Total Energies TADI: A test center with international reach in Lacq [Online] // ETABLISSEMENT PAU LACQ. - 2025. - 2 17, 2025. - https://cstjf-pau.totalenergies.fr/en/our-expertise/leveraging-digital-innovation/tadi-test-center-international-reach-lacq.
Wang J.L. [et al.] Multiscale Methane Measurements at Oil and Gas Facilities Reveal Necessary Frameworks for Improved Emissions Accounting [Journal] // Environmental Science & Technology. - 2022. - 20 : Vol. 56. - pp. 14743-14752.